Looping Formation During Colonoscopy A Simulation

Charles R. Welch and John D. Reid
Department of Mechanical & Materials Engineering
University of Nebraska-Lincoln
W342 NH (0526), Lincoln, NE 68588 USA

Abstract

A simulation of a loop formation during colonoscopy is attempted using LS-DYNA®. The tissue is comprised of a Mooney-Rivlin rubber model adjusted iteratively to somewhat match raw force-displacement data of small intestine tissue. After finding adequate parameters for friction and damping coefficients, the scope is advanced into a colon model in the simulation and loop formation appears. Whether the loop formation obtained through simulation is realistic remains to be determined due to lack of good test data.

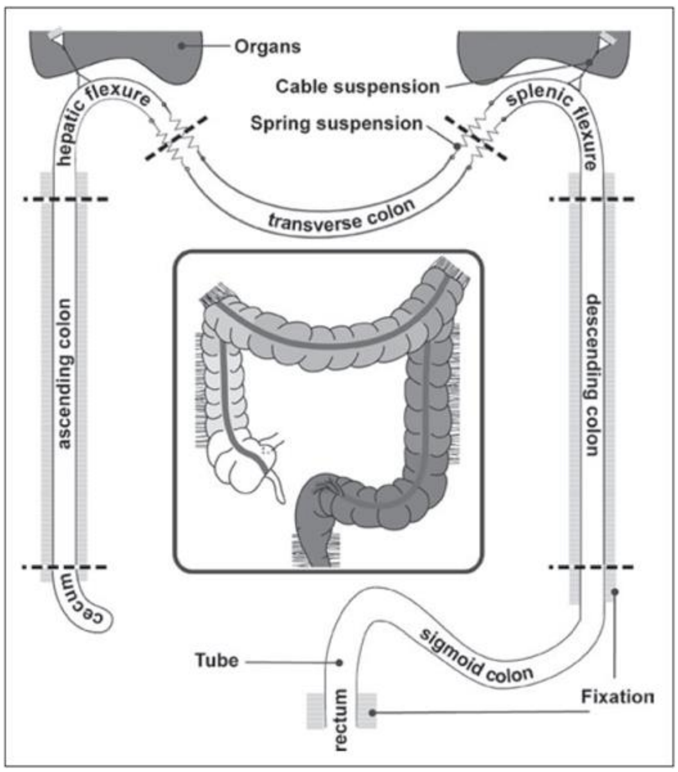

Figure 1. Colon Physical Constraints as Developed by Loeve, et al.

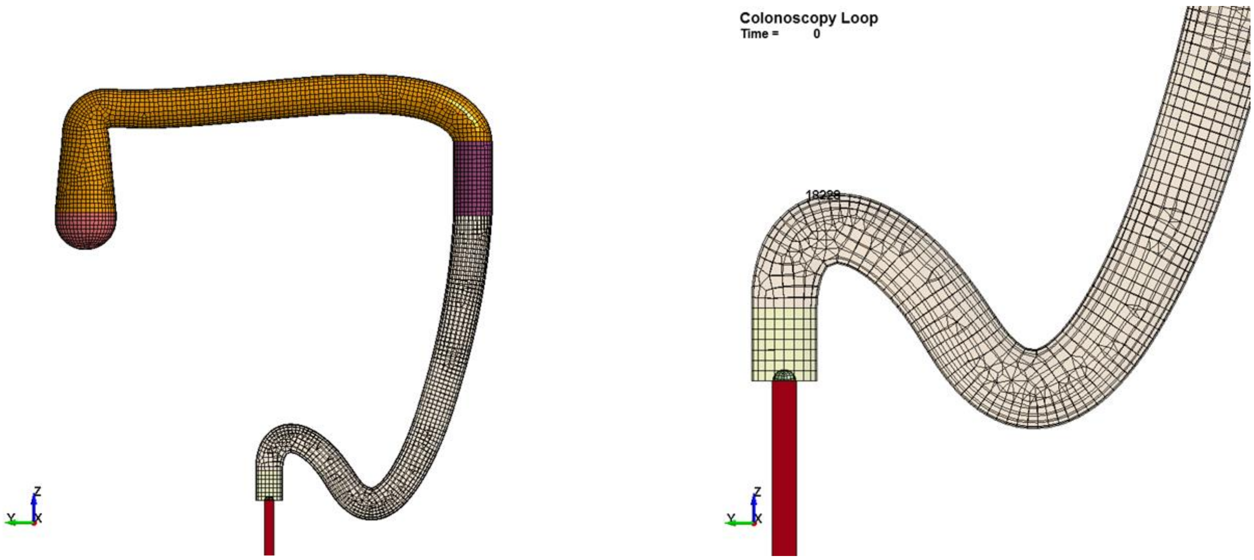

Figure 2. Colon Model

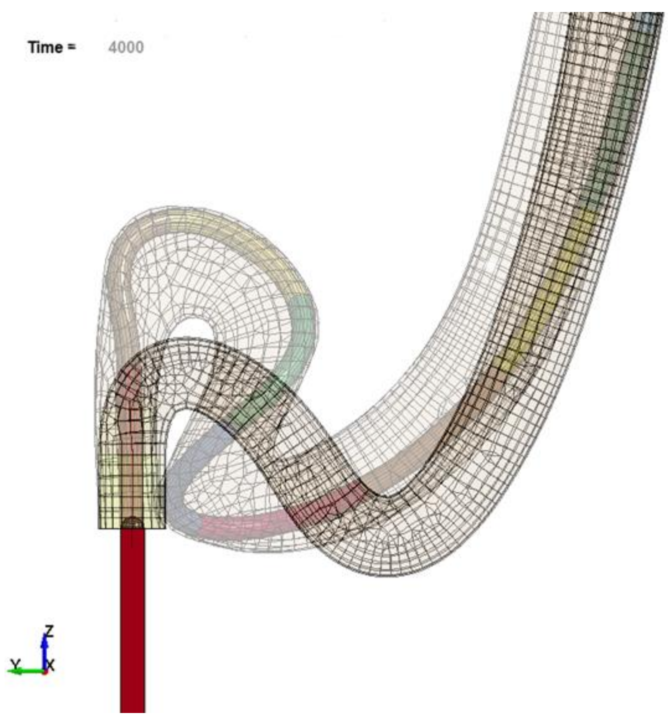

Figure 3. Loop Formation

Introduction

Loop formation is a common event that occurs frequently in routine colonoscopy. While it does not often affect the diagnosis performed during the procedure, looping often causes patients discomfort and pain. Looping most often occurs in the sigmoid colon as the colonoscope (‘scope’) is slowly inserted. A model for this event is created and simulation is attempted.

Models of the mechanical components of a colon have already been attempted in [1] although it is for a simple mechanical analysis and not for finite element analysis. The researchers in this study fix the rectum, ascending colon, and descending colon. This fixation represents the various ligaments and connecting tissue surrounding the colon. A cable model is used to represent the constraints at the hepatic and splenic flexures. As this simulation only involves the sigmoid colon, the cable models at each flexure are not included, but the three sections of colon are fixed instead. Other organs and tissue surrounding the colon are represented by damping the movement of the colon itself [1].

During colonoscopy, the colon is insufflated to separate the folds in the tissue to both allow the scope to move and to allow the colon to be exposed for diagnosis. In this model, the colon is pressurized to 9mm Hg, as per results listed in [2].

Modeling the tissue is an important consideration as mechanical properties of biological tissue vary greatly. A preliminary study on porcine tissue is done in [3] which explores the longitudinal and circumferential moduli of the small intestine. Results show that the moduli vary over the length of the small intestine, with a higher circumferential modulus toward the proximal end and a higher longitudinal modulus toward the distal end of the small intestine. The material model discussed is compared directly to raw data used in a uniaxial test from the aforementioned study although it is unclear how accurately the data represents mechanical properties of the large intestine since it was primarily a characterization of small intestine tissue.

Friction and damping coefficients are iteratively determined using the simulation. Each is changed until a desired loop formation is achieved.

Ideally, the colon model used in this experiment will be used as a future tool to compare alternative colonoscopy procedures to the traditional scopes to show that looping can be avoided altogether.

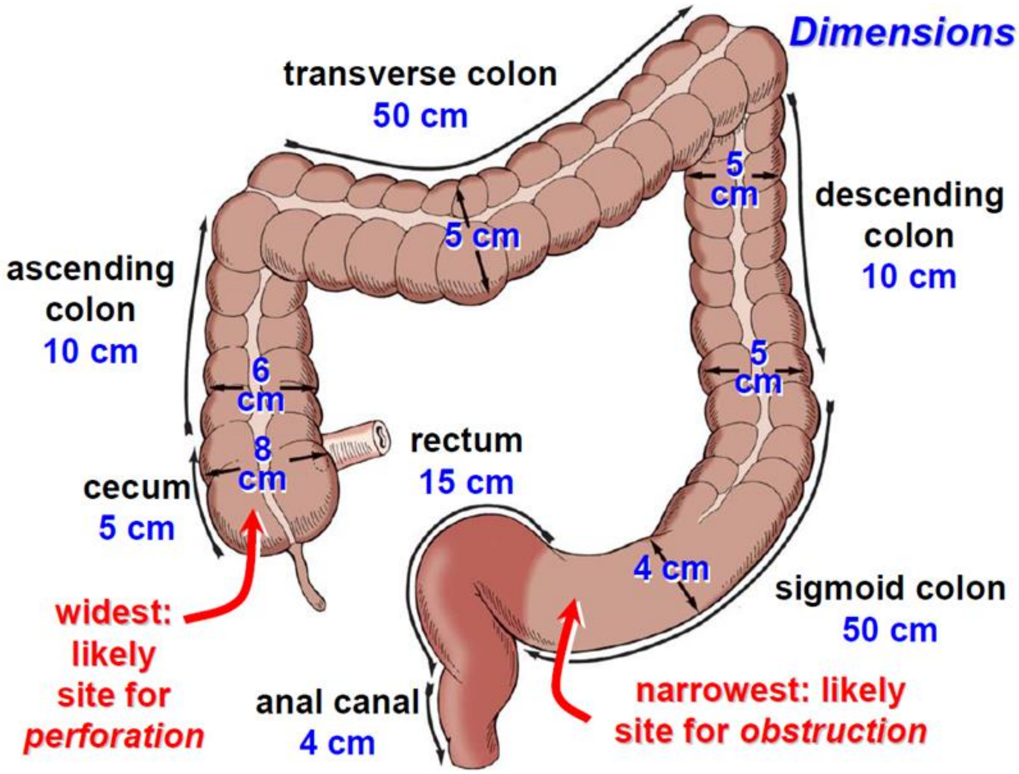

Figure 4. Colon dimensions and general shape [4]

Model Setup

Colon Model

Interpretations on colon geometry and orientation are ambiguous. In [4], dimensional callouts to each section of the colon are given (see Figure 4). Other research shows that the colon wall thickness varies throughout from 0.2mm to 5mm [5]. The dimensions shown in Figure 1 are used in this colon model with an average wall thickness of 2mm used throughout. Curvature and relative location of the colon are left up to interpretation; for this simulation the spline used to create the colon in CAD software is shown in Figure 5.

A model of large intestine constraints was attempted in [1]; the same constraint model is used as a basis for this simulation. In this study, the rectum, ascending colon, and descending colon are all fixed as a representation of the ligaments and connecting tissue surrounding them (see Figure 6). Single point constraints (*BOUNDARY_SPC) are used to fix the nodes at the free end of the rectum and all of the nodes comprising the ascending colon and descending colon.

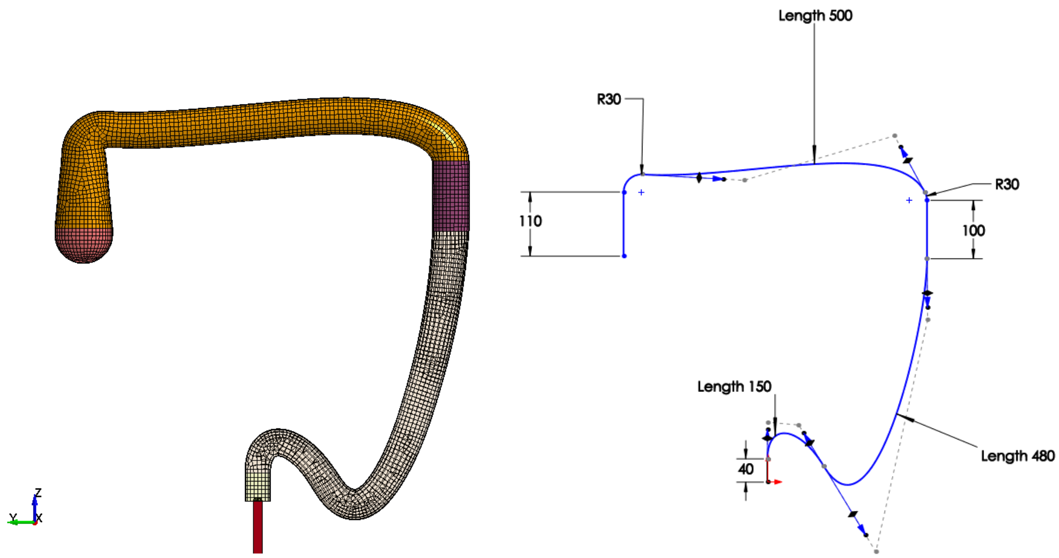

Figure 5. Colon Geometry and Spline Used for Colon Model

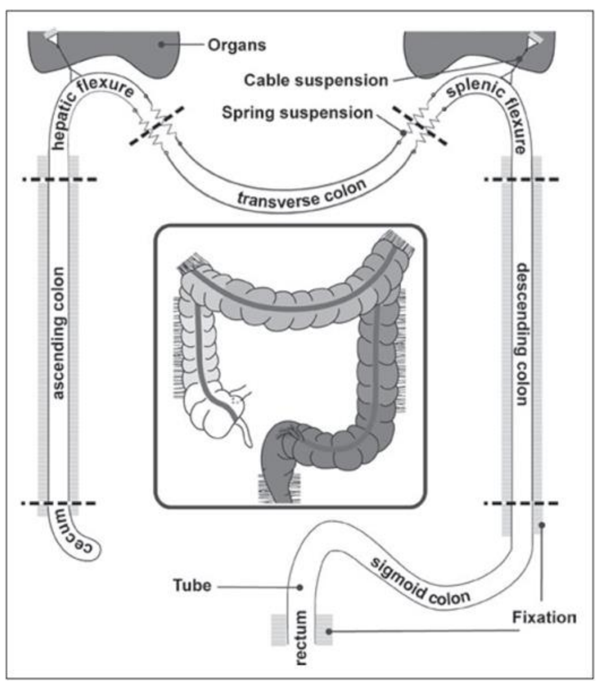

Figure 6: Constraints as per Model Developed by Loeve, et al [1]

Insufflation pressure varies between 9mm Hg and 57mm Hg through the average run and is adjusted manually by the operator in traditional colonoscopy [2]. Insufflation pressure is increased to separate folds in the tissue in order to expose all sections of the large intestine. In this study, the colon was created without folds in the tissue, so the insufflation pressure is set to a minimum, 9mm Hg (1.2e-6 GPa as per units used in k-file). Pressurization is applied with the *AIRBAG command with the simple volume option included. Use of this keyword not only allows for application of pressure to the inside of the colon, but it also allows for damping via the mass weight damping (MWD) parameter associated with the *AIRBAG keyword. Damping allows for representation of the surrounding fluids and tissue that “damp” the movement of the colon when the scope is inserted.

Since the colon wall is modeled as smooth (without folds) in this simulation, the coefficients of friction can be increased to represent the folds in the tissue that prevent advancement of the scope. In this model, automatic single surface contacts are used with SOFT parameter set to 1.

Scope Model

The scope used in this simulation was modeled after conventional colonoscopes, with a diameter of 12.8mm [8]. These conventional scopes vary in flexibility along the length of the insertion tube, being more flexible at the distal end and less flexible toward the end [6]. The scope was simplified in this simulation and defined as a Blatz-ko rubber model with the bulk modulus iteratively increased until looping began to form. This occurred with the bulk modulus set to 1 MPa and the density set to 20.0e-6 kg/mm^3.

Further experimentation can be done to classify the material in the scope. For example, a simple cantilever test of the scope can be performed and replicated in a simulation to verify the modulus properties and density; however, that was not performed in this study. Another check can be done by comparing the radius of curvature (Figure 7). This can be found experimentally by fixing one end of the scope and applying a moment to the other in a simulation and comparing the results to the test.

Figure 7: Natural Radius of Curvature of the Olympus CF Type 130 Colonoscope

Tissue Material Model

Preliminary characterization of small intestine tissue was performed in [3] where a section of tissue was pulled in the longitudinal direction to measure force and deflection. A single shell element (with the same cross-section and length) was pulled in a simulation and compared to the raw test data. The raw data showed that the maximum deflection experienced by the tissue was 19mm. This displacement value was used as a basis for the simulation; the shell element was displaced 19mm and force was recorded.

Material properties for the tissue consisted of a Mooney-Rivlin rubber model that requires density, Poisson's ratio, and two constants (A and B), that make up the shear modulus (shear modulus = 2(A+B)). In order to characterize the material, and initial guess was given at A = 2.8e-5 and B = 1.2e-5 and the numbers were progressively cut in half until the force-deflection curve was somewhat close to the raw test data. Different iterations are compared to the test data in Figure 8. At A = 3.0e-6 and B = 1.0e-6, the simulation curve passed through the test data curve, and these parameters were used in the material model representing the colon tissue.

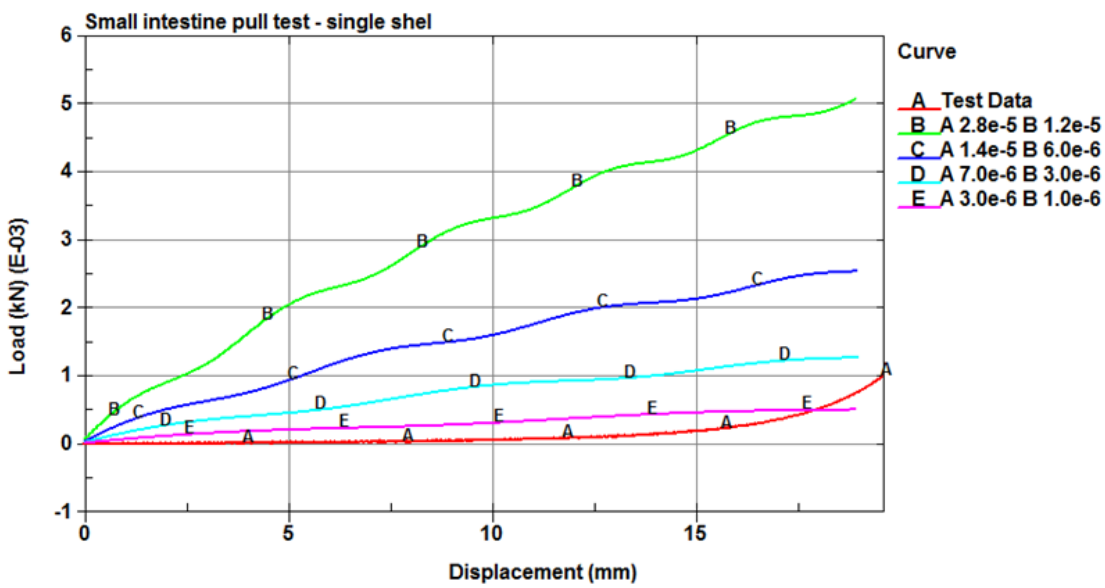

Figure 8. Force-Deflection Curves: Simulated versus Test

Considerations

While the material properties largely influenced the results of the simulation, other parameters also had a big influence. Friction coefficients proved to be a key parameter in obtaining loop formation. This likely represents the irregularities and folds in the tissue that prevent the scope from advancing. When the friction coefficients were increased, the scope had more difficulty advancing through the first two turns of the colon, resulting in higher displacement values and greater loop formation.

Damping also played an important part in loop formation. With little to no damping, the scope would essentially run into the colon wall and take the first two turns with it. As damping was added, the scope was able to bend around that first turn. Damping appeared to be sufficient at MWD = 2.0kg. The difference is shown in Figure 9.

Figure 9. Left - MWD = 0.005kg, Right - MWD = 2.0kg

Another important consideration is how the geometry of the colon is defined. If the first two turns are too "loose", the scope will have an easy time advancing; however, if the first two turns are "tight", the scope will bind up at the second turn and looping will be more likely to occur. Different iterations of colon geometry were made and the evolution throughout this simulation is shown in Figure 10.

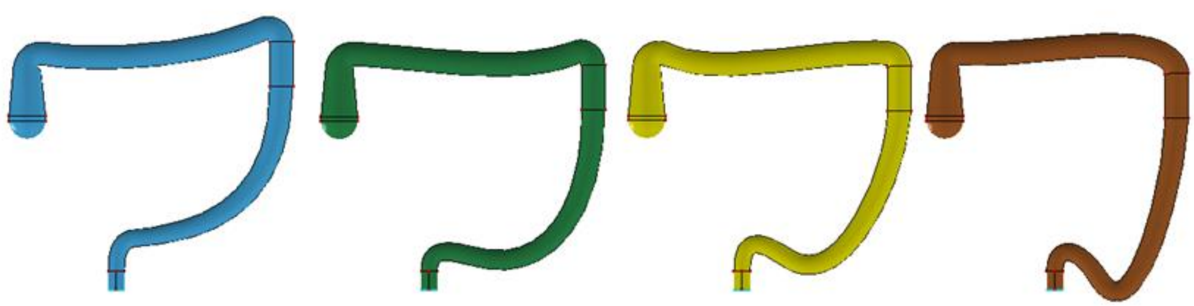

Figure 10. Evolution of Colon Geometry from Simulation Iterations

Results

Various iterations were recorded to find the values for each of the parameters that seemed to affect looping formation the most: material properties, friction coefficients, damping (MWD) values, and colon geometry. These values gave the best result for loop formation:

- Mooney-Rivlin constants
  - A = 3.0e-6
  - B = 1.0e-6
- Friction coefficients
  - Static (fs) = 0.06
  - Dynamic (fd) = 0.06
- Damping
  - MWD = 2.0kg
- Colon geometry
  - Tight first and second turn

A simulation with these constants resulted in loop formation shown in Figure 11. Node 18228 (identified in Figure 12) was tracked using the trace post-process to measure displacement. The resultant displacement of this node is recorded in Table 1. Maximum deflection occurs at the end of the simulation (73.5mm). Since the maximum deflection occurs at the end of the simulation it seems probable that the loop will continue to grow once the scope tip advances through the splenic flexure.

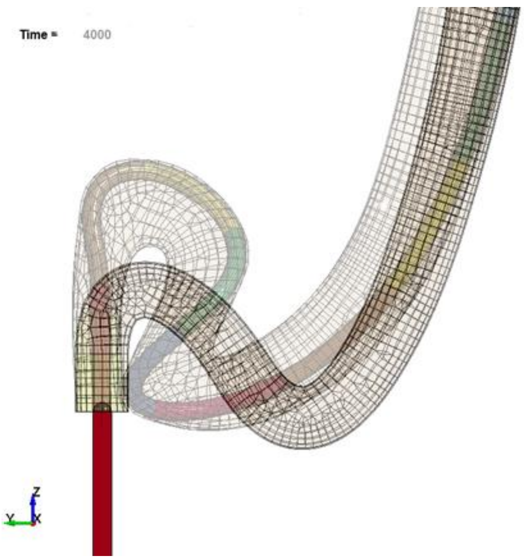

Figure 11. Loop Formation

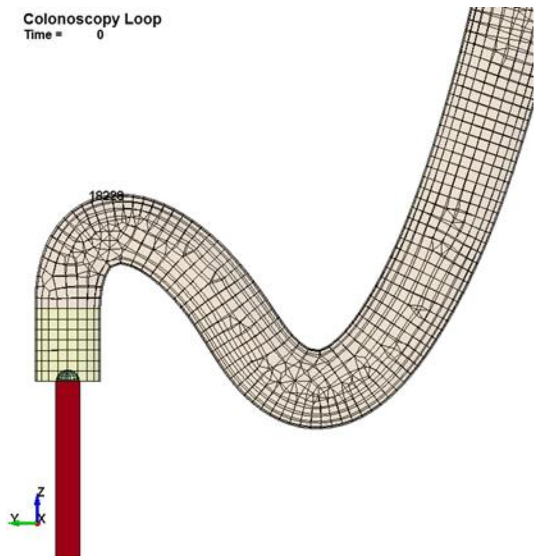

Figure 12. Node 18228 Location

Table 1. Resultant Displacement of Node 18228 (mm)

Node 18228			
x-disp	y-disp	z-disp	Resultant
0.00E+00	0.00E+00	0.00E+00	0
-1.28E+00	4.78E+00	9.37E+00	10.59596
-1.25E+00	7.29E+00	1.07E+01	13.01428
-3.33E-01	1.98E+00	1.68E+01	16.96188
-5.85E-01	-1.35E+00	2.06E+01	20.61968
-7.27E-01	-3.32E+00	2.04E+01	20.72563
-7.95E-01	-5.59E+00	1.41E+01	15.18636
-1.14E+00	-3.53E+00	1.75E+01	17.86656
-5.14E-01	1.13E+00	3.16E+01	31.62755
5.25E-02	5.88E+00	4.73E+01	47.61555
3.02E+00	7.79E+00	5.70E+01	57.60996
7.37E+00	9.47E+00	6.18E+01	62.95914
1.13E+01	1.00E+01	6.31E+01	64.92609
1.46E+01	1.18E+01	6.56E+01	68.25955
1.76E+01	1.40E+01	6.84E+01	72.01113
1.98E+01	1.61E+01	6.70E+01	71.71504
1.84E+01	1.55E+01	6.38E+01	68.16317
1.94E+01	1.54E+01	6.05E+01	65.42232
2.14E+01	1.60E+01	5.91E+01	64.89501
2.41E+01	1.59E+01	6.07E+01	67.21988
2.76E+01	1.05E+01	6.73E+01	73.52951

Discussion

Loop formation appears as a result of the simulation, but is it realistic? Magnetic endoscope images (MEI) have been obtained in medical school textbooks but without dimensions and completely void of colon layout and relative location (see Figure 13) [7]. Besides comparing the shape of the loop to MEIs, another way to verify if a loop is consistent with the real-life event is to compare resultant displacement of the sigmoid colon, however, no research has been found on the displacement of the sigmoid colon caused by looping. That the simulation results prove to be realistic remains to be determined due to the lack of good test data.

Further work remains to improve the simulation. A material model for the scope can be done similar to that of the material model for the colon tissue discussed previously. More sections of the scope can be inserted into the colon to see if the loop continues to grow as the tip of the scope contacts the splenic flexure. Flexibility of the scope can also be varied along the length of the insertion tube by varying the bulk modulus at different sections of the scope.

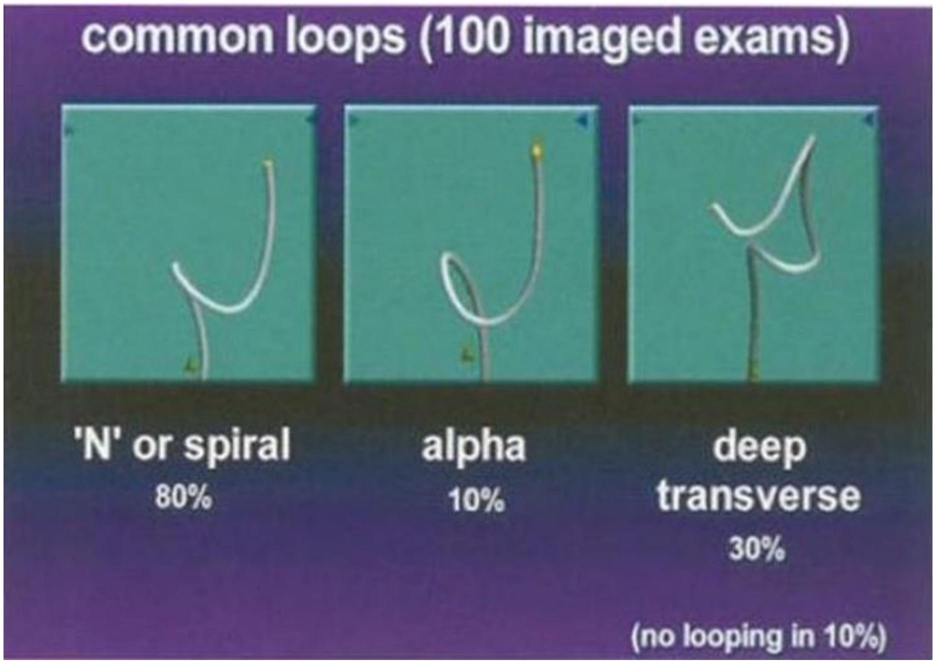

Figure 13. Magnetic Endoscope Images of Different Loop Formations

Conclusion

Loop formation during colonoscopy was attempted in a simulation. After iteratively testing for different parameters and developing a material model for the tissue, the simulation appeared to successfully form a small loop. Whether this loop formation is realistic or not is yet to be determined as future work could provide more evidence for realistic behavior.

Acknowledgments

The authors appreciate LSTC for making LS-DYNA readily available for this research. A special thanks to Dr. Carl Nelson for help in formulating the idea for this simulation and to Dr. Benjamin Terry for providing the test data for the intestinal tissue. The simulation work performed for this project was completed utilizing the Holland Computing Center of the University of Nebraska–Lincoln.

References

[1] Loeve, A., Fockens, P., Breedveld, P. *Mechanical analysis of insertion problems and pain during colonoscopy.* Can J Gastroenterol Vol 27 No 5. May 2013.

[2] Kozarek, R.A., et al., *Air-pressure-induced colon injury during diagnostic colonoscopy.* Gastroenterology. 78(1): p. 7-14.

[3] Terry, B., Wang, X., Schoen, J., Rentschler, M. *A preconditioning protocol and biaxial mechanical measurement of the small intestine*. International Journal of Experimental and Computational Biomechanics. Vol 2 No 4. 2014.

[4] Whitmer, Lawrence M. *Clinical Anatomy of the Large Intestine*. Centers for Osteopathic Research & Education. Jan 23, 2007.

[5] Wiesner, W., Mortele, K.J., Ji, H., Ros, P.R. *Normal colonic wall thickness at CT and its relation to colonic distension.* J Comput Assist Tomogr. 2002 Jan-Feb; 26(1):102-6.

[6] Wayne, J.D., Rex, D.K., Williams, C.B. *Flexibility.* Colonoscopy: Principles and Practice. Wiley. 2009.

[7] Chapman, A.H. *Radiology and Imaging of the Colon*. Section 28.4.1.1 pg. 304.

[8] ASGE Technology Committee Shyam Varadarajulu, Subhas Banerjee, Bradley A. Barth, David J. Desilets, Vivek Kaul, Sripathi R. Kethu, Marcos C. Pedrosa, Patrick R. Pfau, Jeffrey L. Tokar, Amy Wang, Louis-Michel Wong Kee Song, Sarah A. Rodriguez. *GI Endoscopes*. Gastointestinal Endoscopy. Vol. 74 No 1. 2011.